Contents lists available at ScienceDirect

Engineering Structures

Bond behaviour of austenitic stainless steel reinforced concrete

Musab. Rabi[a,b,*], K.A. Cashell[b], R. Shamass[c], Pieter Desnerck[d]

[a] Dept of Civil Engineering, Jerash University, Jordan
[b] Dept of Civil and Environmental Engineering, Brunel University London, UK
[c] Division of Civil and Building Services Engineering, School of Build Environment and Architecture, London South Bank University, UK
[d] Dept of Engineering, University of Cambridge, UK

ARTICLE INFO

ABSTRACT

Stainless steel reinforced concrete has seen a large increase in usage in recent years, in response to the ever-increasing demands for structures and infrastructure to be more durable, efficient and sustainable. Currently, existing design standards advise using the same design rules for stainless steel reinforced concrete as traditional carbon steel reinforced concrete, owing to a lack of alternative information. However, this is not based on test or performance data. As such, there is a real need to develop a full and fundamental understanding of the bond behaviour of stainless steel reinforced concrete, to achieve more sustainable and reliable design methods for reinforced concrete structures. This paper investigates the bond behavior of stainless steel reinforced concrete and compares the performance to traditional carbon steel reinforced concrete, through experimental testing and analysis. It also compares the results to existing design rules in terms of bond strength, anchorage length and lap length. It is shown that stainless steel rebar generally develops lower bond strength with the surrounding concrete compared with equivalent carbon steel reinforcement. Moreover, it is shown that existing design codes are very conservative and generally underestimate the actual bond strength by a significant margin. Therefore, following detailed analysis, it is concluded that current design rules can be safely applied for stainless steel rebar, although more accurate and efficient methods can be achieved. Hence, new design parameters are proposed reflecting the bond behaviour of stainless steel rebar, so that more efficient designs can be achieved. Moreover, a summary of recommendations for the codes of practice is provided.

1. Introduction

In response to growing demands for civil engineering structures and infrastructure to be more durable, sustainable and efficient, stainless steel has emerged as a very attractive material for many applications. It is available in several different forms including sheet, plate and bar products as well as structural sections. Stainless steel elements are corrosion resistant with low or negligible maintenance requirements over a long life cycle, and also offer excellent strength, ductility, toughness, recyclability and fatigue properties. Of course, they are more expensive than traditional carbon steel and therefore must be used efficiently and in appropriate applications.

There are five main categories of stainless steel which are classified according to their metallurgical structure, including the austenitic, ferritic, duplex, martensitic and precipitation hardened grades. Each of these groups provides their own unique properties and corrosion resistance characteristics. The austenitic and duplex grades are most common in structural applications, including for stainless steel

reinforcement, owing to their excellent corrosion resistance associated with the outstanding mechanical properties [1–3]. One of the most important chemical elements in all stainless steel alloys is chromium which provides the corrosion resistance through the formation of a thin chromium oxide film on the surface of the material in the presence of oxygen, resulting in a passive protective layer [4]. Until recently, stainless steel was commonly used in load-bearing applications as bare structural sections such as beams and columns. However, a relatively new application for stainless steel is as reinforcement in concrete structures.

Reinforced concrete is one of the most common structural solutions found in construction, and is used in a wide range of applications such as bridges, tunnels, multi-story buildings. It is popular because it provides an economic, efficient and versatile solution and there is plenty of guidance and performance criteria available for designers. However, one of the fundamental challenges that is experienced by reinforced concrete structures is corrosion of the reinforcement, especially for members which are exposed to harsh environments such as in coastal,

* Corresponding author.
  E-mail address: Musab.rabi@jpu.edu.jo (M. Rabi).

marine or industrial settings [5]. For concrete structures reinforced with traditional carbon steel and subjected to aggressive or polluted environments, corrosion cannot be avoided. This results in a significant reduction in the lifetime of the structure and increases the monitoring and maintenance costs associated with carbonation and deterioration of concrete and corrosion of reinforcement.

There is a huge demand to improve the durability and life-cycle of reinforced concrete structures. The typical approach is to increase the concrete cover, to control the alkalinity of concrete, to adjust the ingredients and composition of the concrete, or to use cement inhibitors [6]. However, in aggressive conditions, these measures may not be sufficient to prevent a corrosion problem. In this context, the use of stainless steel reinforcement represents an ideal solution for exposed reinforced concrete structures. Replacing the traditional carbon steel reinforcement with stainless steel improves the expected life time of these structures and may also significantly reduce the costs associated with expensive inspection and rehabilitation works [7,8]. Although the initial cost of stainless steel reinforcement is relatively high compared to that of traditional carbon steel, the use of stainless steel reinforcing bar can reduce the overall maintenance costs up to 50% [9].

The focus in this paper is on the bond relationship between the rebars and the surrounding concrete. It builds on previous work which studied the more fundamental constitutive material properties of stainless steel reinforcement [10,11]. Stainless steel exhibits a quite different constitutive stress-strain response compared with carbon steel in that it does not have the typical yield plateau and also develops significant strain hardening with excellent ductility. Bond is clearly a key property that needs to be considered when assessing the response of reinforced concrete and composite structures. It has a direct influence on the structural performance and inadequate bond can cause many different issues including ineffective anchorage, widespread cracking of the concrete and excessive deflections or rotations. Thus, having an accurate and realistic knowledge of the bond strength is imperative especially for the serviceability limit state. However, it is a relatively complex phenomenon owing to the many inter-related parameters which govern its development. Amongst the most influential parameters are the quality of the concrete and the surface geometry of the reinforcing bar. For example, voids that develop in the concrete during the casting and hardening process may result in a reduction in the local bond strength [12]. Other factors which influence the development of bond strength include the cover distance, the clear space between adjacent bars, the number and size of bar layers and the direction of casting with respect to the orientation of the bars [13]. The influence of bar stresses on the bond behaviour is relatively small as long as the bar does not yield. However, once it yields, the transverse forces between the bars and the concrete decrease resulting in a reduction in the bond stress-slip response [13].

Bond stress is developed by an adhesive action combined with frictional forces and the mechanical interlocking of the concrete against the bar-surface deformities. For plain, smooth bars, the development of bond relies primarily on adhesion and friction although there may be some interlocking if the bar surface is rough. Therefore, the use of ribbed reinforcement rather than plain bars significantly increases the bond strength that develops. The relative rib area (f_P), which is a dimensionless property, is used as indication of the quality of the rib geometry according to EN 15630-1 [14]. A typical value in the range of 0.05–0.10 for the relative rib area is appropriate for generating adequate bond strength and providing a good service-load performance. It has been shown that bond strength increases linearly with the increase of relative rib area [15]. The relative rib area is calculated as shown in Eq. (1):

$$f_P = \frac{1}{\pi.\phi.} \sum_{i=1}^{n} \frac{F_{p,i}\sin\beta_i}{c_i} \tag{1}$$

in which F_P is the area of the longitudinal section of a single rib, i is the

number of series of transverse ribs, ϕ is the bar diameter, n is the number of indentation rows and c and β are the rib spacing and rib inclination, respectively.

Current design standards such as Eurocode 2 [16] and MC2010 [17] do not include specific rules for stainless steel reinforced concrete, and generally suggest using the same criteria as for traditional carbon steel reinforced concrete. There has been considerable research into stainless steel reinforcement, especially in recent years, but most has focussed on the corrosion behaviour (e.g. [18–22]), with limited research on the bond behavior in a corrosive environment (e.g. [7,23]). There have been very few studies in to the bond behavior of stainless steel rebar, and these have even resulted in inconclusive results with one study showing that the bond developed by some austenitic and duplex stainless steel bars is lower than for similar carbon steel reinforcement (e.g. [24]) whilst other publications have shown the opposite finding (e.g. [25–26]). Accordingly, the work presented in the current paper aims to investigate the bond behavior of stainless steel rebar encased in concrete with reference to that of traditional carbon steel, and suggest suitable values which can be used in design. In addition, the applicability of current bond design rules in Eurocode 2 and MC2010 in terms of bond strength, anchorage length and lap length, is examined. Accordingly, the paper proceeds with a background of the information currently available in design standards, following by a detailed description and analysis of a pull-out test experimental programme involving both stainless steel and carbon steel rebars. Finally, a suitable bond-slip model for stainless steel reinforcement is proposed.

2. Design codes

The bond strength that develops between steel reinforcement and the surrounding concrete is an influential property in the behaviour of reinforced concrete, as it governs the composite action and hence crack development, anchorage of the bars in the concrete and also the transfer of stresses at laps. Accordingly, international design standards such as Eurocode 2 [16] and the Model Code 2010 [17] include design predictions for the bond strength, and also these other important performance criteria. Of course, as stated before, bond is a complex and multi-faceted phenomena, so different design codes adopt various simplifications in order to aid designers. In this section, the provisions provided in Eurocode 2 and Model Code 2010 are summarised, as well as their key differences.

2.1. Eurocode 2 (2004)

In Eurocode 2, to obtain the design anchorage length and lap length, the design bond strength (f_{bd}) must first be calculated, followed by the basic anchorage length ($l_{b,rqd}$). The design bond strength is determined as follows:

$$f_{bd} = 2.25\eta_1\eta_2 f_{ctd} \tag{2}$$

In this expression, η_1 is a coefficient related to the bond condition and the bar position during casting, and a value of unity represents a good bond condition whilst 0.7 represents all other conditions. η_2 is a coefficient related the bar diameter (ϕ) and is taken as unity when the diameter is less or equal to 32 mm and is otherwise determined using Eq. (3):

$$\eta_2 = \frac{132 - \phi}{100} \quad \text{for } \phi > 32 \text{ mm} \tag{3}$$

The tensile concrete strength (f_{ctd}) is obtained as a function of the characteristic concrete compressive strength (f_{ck}) as given in Eq. (4):

$$f_{ctd} = 0.21(f_{ck})^{2/3} \quad \text{for concrete strength} \leqslant \text{C60/75} \tag{4}$$

Eurocode 2 states that the tensile concrete strength is limited for concrete class C60/75, unless it can be verified that the bond strength can be increased above this limit.

The basic anchorage length $I_{b,rqd}$ is determined as:

$$I_{b,rqd} = \frac{\phi\sigma_{sd}}{4f_{bd}} \tag{5}$$

where σ_{sd} is the design stress in the reinforcing bar.

The design anchorage length (I_{bd}) is calculated using Eq. (6):

$$I_{bd} = \alpha_1\alpha_2\alpha_3\alpha_4\alpha_5 I_{b,rqd} \geq I_{b,min} \tag{6}$$

In this expression, $I_{bd,min}$ is the minimum accepted value for the design anchorage length, determined as:

$$I_{b,min} \geq \max\{0.3I_{b,rqd}; 10\phi; 100 \text{ mm}\} \text{ for anchorage in tension} \tag{7}$$

α_1 and α_2 are coefficients related to the form of bar and the minimum cover distance, respectively, and α_3, α_4 and α_5 are coefficients related to the condition of confinement. These parameters are obtained as follows for reinforcement that is in tension:

$\alpha_1 = 1$ for straight bars.

$\alpha_2 = 1 - 0.15(c_d - \phi)/\phi \geq 0.7$ and ≤ 1.0

α_3, α_4, and α_5 are taken as unity if there is no confinement provided by transverse reinforcement, welded transverse reinforcement and transverse pressure, respectively.

The design lap length (I_0) is calculated using Eq. (8):

$$I_0 = \alpha_1\alpha_2\alpha_3\alpha_5\alpha_6 I_{b,rqd} \geq I_{0,min} \tag{8}$$

In this expression, ($I_{0,min}$) is the minimum accepted value for the design lap length, determined as:

$$I_{0,min} \geq \max\{0.3\alpha_6 I_{b,rqd}; 15\phi; 200 \text{ mm}\} \tag{9}$$

where α_6 is coefficient related to the percentage of the lapped bars relative to the total cross-section area which is taken as 1 for percentage lower than 25%.

2.2. Model Code 2010 (2013)

The Model Code 2010 (it will be referred to hereafter as MC2010) provides guidance for the design of reinforced and prestressed concrete by the International Federation for Structural Concrete (known as the fib, or Fédération internationale du béton). Similar to Eurocode 2, MC2010 requires calculation of the design bond strength (f_{bd}) in order to establish the required anchorage and lap lengths. It is noteworthy that the symbols used in this section may vary from those employed in the MC2010, but are changed herein to be consistent with the earlier discussions.

The bond strength is determined as:

$$f_{bd} = (\alpha_2 + \alpha_3)f_{bd,0} \tag{10}$$

where α_2 and α_3 represent the influence of passive confinement from the concrete cover and from transverse reinforcement. These values are found from:

$\alpha_2 = (c_{min}/\phi)^{0.5} \cdot (c_{max}/c_{min})^{0.15}$ for ribbed bars;
$\alpha_2 = (c_{min}/\phi)^{0.8} \cdot (c_{max}/c_{min})^{0.15}$ for epoxy-coated or plain bars; and

$\alpha_3 = K_d \cdot (K_{tr} - \alpha_t/50)$

c_{max} and c_{min} are cover parameters, α_t is 0.5 for bars with a diameter up to 25 mm and K_d and K_{tr} are effectiveness factors dependent on the reinforcement details and the density of the transverse reinforcement relative to the anchored or lapped bars, respectively. K_d and K_{tr} are taken as zero in the case where no transverse reinforcement is provided.

$f_{bd,0}$ is the basic bond strength which is a function of the characteristic concrete compressive strength (f_{ck}) and is calculated using Eq. (11):

$$f_{bd,0} = \eta_1\eta_2\eta_3\eta_4(f_{ck}/25)^{0.5} \tag{11}$$

Table 1
Determining η_4 coefficient.

Characteristic strength of the reinforcement f_{yk} (MPa)	η_4
400	1.2
500	1.0
600	0.85
700	0.75
800	0.68

In this expression, the following values are employed for the various constants:

$\eta_1 = 1.75$ for ribbed bars;
$\eta_2 = 1$ for good bond conditions;
$\eta_3 = 1$ for $\phi < 25$; and
η_4 represents the characteristic strength of the reinforcement (f_{yk}) which is being anchored or lapped and is obtained from the values given in Table 1.

The design anchorage length (I_b) is calculated as presented in Eq. (12):

$$I_b = \frac{\phi\sigma_{sd}}{4f_{bd}} \geq I_{b,min} \tag{12}$$

In this expression, $I_{b,min}$ is the minimum accepted value for the design anchorage length, determined as:

$$I_{b,min} > \max\left\{\frac{0.3\phi f_{yd}}{4f_{bd}}; 10\phi, 100 \text{ mm}\right\}$$

where σ_{sd} is the stress in the bar to be anchored by bond over the anchorage length and is obtained as follows:

$\sigma_{sd} = \alpha_1 f_{yd}$

$$\alpha_1 = A_{s,cal}/A_{s,ef} \tag{13}$$

In these expressions, f_{yd} is the design yield strength of the reinforcement, and $A_{s,cal}$ and $A_{s,ef}$ are the required area of reinforcement determined in design and the actual area of reinforcement as provided, respectively.

The design lap length (I_0) is calculated as given in Eq. (14):

$$I_0 = \alpha_4\frac{\phi f_{yd}}{4f_{bd}} \geq I_{0,min} \tag{14}$$

In this expression, $I_{0,min}$ is the minimum accepted value for the design lap length, determined as:

$$I_{0,min} > \max\left\{\frac{0.7\phi f_{yd}}{4f_{bd}}; 15\phi, 200 \text{ mm}\right\}$$

where α_4 is typically taken as unity but it can be reduced to 0.7 when the calculated stress in the bar at the ultimate limit state throughout the lap length does not exceed 50% of the reinforcement characteristic strength.

2.2.1. Bond stress-slip model

In addition to the design bond strength and anchorage length values, MC2010 also provides two different design bond stress-slip relationships. The designer selects the appropriate relationship to employ based on the failure mode, either failure through bond or confinement. The general bond stress-slip model is shown in Fig. 1, and has four main stages for pullout failure. Firstly, and with reference to Fig. 1, while the slip (s) is less than s_1, the bond stress is developing as the ribs on the rebars bear against the concrete. This stage is characterized by local crushing and micro-cracking of the concrete. Then, in the second stage when $s_1 < s < s_2$, the bond strength plateaus at the maximum value of τ_{bmax}. This represents the bond capacity which is influenced mainly
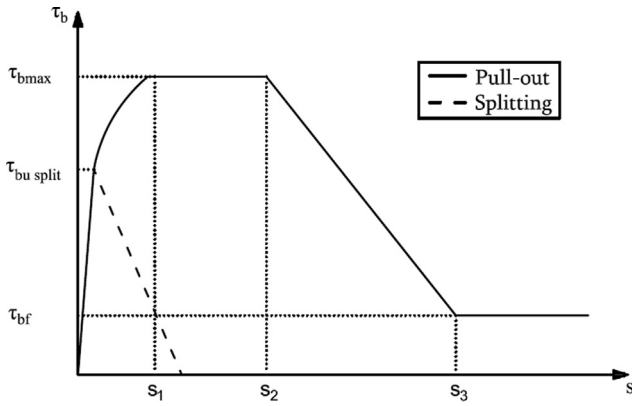
Fig. 1. Bond stress-slip model in MC2010 [17].

by the degree of confinement. This is followed by the third stage ($s_2 < s < s_3$) in which the bond stress decreases as the interlocking mechanical bonds between the ribs and concrete reduce. Finally, when $s > s_3$, the constant residual bond level (τ_{bf}) is reached, which is mainly comprised of frictional resistance.

The bond-slip relationship provided in MC2010 describes the bond stress (τ_b) as a function of the relative displacement (s), as presented in Eqs. (15)–(18) for the four stages, respectively:

$$\tau_b = \tau_{bmax}(s/s_1)^\alpha \quad \text{for} \ \ 0 \leq s \leq s_1 \tag{15}$$

$$\tau_b = \tau_{bmax} \quad \text{for} \ \ s_1 \leq s \leq s_2 \tag{16}$$

$$\tau_b = \tau_{bmax} - \frac{(\tau_{bmax} - \tau_{bf})(s - s_2)}{s_3 - s_2} \quad \text{for} \ \ s_2 \leq s \leq s_3 \tag{17}$$

$$\tau_b = \tau_{bf} \quad \text{for} \ \ s_3 \leq s \tag{18}$$

The parameters required in these equations are given in Table 2, where τ_{bf} is the residual bond stress, c_{clear} is the clear distance between adjacent ribs and f_{cm} is the mean cylinder concrete compressive strength and is calculated using Eq. (19):

$$f_{cm} = f_{ck} + 8 \tag{19}$$

It is noteworthy that the values given in Table 2 are for a "good" bond conditions and are only valid for ribbed rebars in which the tensile strain in the rebar is lower than its yield limit.

The other bond stress-slip model given in MC2010 is for splitting failure, and in this, the bond strength ($\tau_{bu,split}$) is determined as follows:

$$\tau_{bu,split} = 6.5\eta_2 \left(\frac{f_{cm}}{25}\right)^{0.25} \left(\frac{25}{\phi}\right)^{0.2} \left[\left(\frac{C_{min}}{\phi}\right)^{0.33}\left(\frac{C_{max}}{C_{min}}\right)^{0.1} + k_m K_{tr}\right] \tag{20}$$

In this expression, k_m represents the efficiency of the confinement from the transverse reinforcement and is taken as zero when no transverse reinforcement is provided.

It is clear from the above discussion that Eurocode 2 provides relatively more simplistic design procedures for predicting the design bond strength compared with the MC2010. However, Eurocode 2 does not provide design guidelines for predicting the bond stress-slip

Table 2
Parameters defining the bond stress-slip relationship.

	Pull-out failure	Splitting failure (unconfined)
τ_{bmax}	$2.5(f_{cm})^{0.5}$	$2.5(f_{cm})^{0.5}$
$\tau_{bu,split}$	–	Eq. (20)
s_1	1.0 mm	$s(\tau_{bu,split})$
s_2	2.0 mm	s_1
s_3	c_{clear}	$1.2\,s_1$
α	0.4	0.4
τ_{bf}	$0.4\tau_{bmax}$	0

relationship. On the other hand, MC2010 includes the influence of important parameters in the design expression such as the confinement effect, presence of transverse reinforcement, form of the indentations, bar size and the characteristic yield strength of the rebar. It is also important to indicate that the bond design rules in Eurocode 2 are derived on the basis of those provided in Model Code. Neither Eurocode 2 nor MC2010 account for the influence that the reinforcement material type has on the bond response.

3. Experimental programme

In order to assess the bond strength between stainless steel reinforcing bars and the surrounding concrete, and to compare the behaviour to carbon steel reinforcement, a series of pull-out tests has been conducted. A further aim of this study is to investigate if the existing design criteria which has been produced on the basis of test results on carbon steel rebar, can be used for stainless steel reinforced concrete. Different concrete strengths and reinforcement grades are included in the test programme. Concrete compression tests and reinforcement tensile tests have also been carried out to determine the characteristic material properties.

3.1. Type of bond test

There are several methods for bond testing suggested in the literature. As is clear from earlier discussions, there are many factors which influence bond strength, and make quantifying this property quite challenging. In addition to the material and geometric properties, bond behaviour is influenced by the details of the test setup which affect the stress conditions in both the concrete and the reinforcement, as well as at the interface. The most widely-used experimental set-ups for evaluating bond strength are the pull-out and beam tests [27]. The beam test requires large specimens and comprises two half-beams which are connected at the bottom by the reinforcing bar and at the top by a hinge. This arrangement closely replicates a real structural arrangement where both the rebar and the surrounding concrete are in tension. On the other hand, the pull-out test is a more straight-forward and simple arrangement in which the reinforcement is embedded at the centre of a cubic or cylindrical concrete specimen, over a controlled bonded length. In this case, the concrete is subjected to compressive stress whilst the reinforcement is in tension. Although this may not represent the actual scenario in reinforced concrete structures, the pull-out test is widely adopted in research because of its capability to provide a reasonable bond response, the relatively low cost and the ease of fabrication [28–29]. They are generally accepted as providing excellent basis for comparison at least, and for understanding the relative influence that different properties, such as reinforcement type, may have on the bond. Therefore, the pull-out test has been selected in the current programme.

3.2. Material properties

3.2.1. Concrete

Three concrete mix designs were selected for the tests to produce C20, C40 and C60 concrete. The concrete was made using high strength Portland cement (known as CEM I 52.5N) and the mix proportions are summarized in Table 3. A super plasticizer was used to enhance the workability of the C60 concrete because of its relatively low water to cement ratio. In addition to the pull-out samples, a number of additional cylindrical specimens with a diameter of 100 mm and height of 200 mm were cast in order to conduct compression tests. These were carried out in accordance with the guidance given in EN 12390-3 [30], as shown in Fig. 2. A total of 18 cylindrical specimens were cast and cured in a water tank at a constant temperature of 21 degrees C for 28 days. Prior to the compressive tests, sulphur capping was applied to both ends of the specimens, as shown in Fig. 3, to avoid any reduction

Table 3
Concrete mix proportions.

Target concrete grade	w/c ratio	Mix proportions (kg/m^3)						Mean compressive strength (MPa)
		Cement (kg/m^3)	Water (kg/m^3)	Sand (kg/m^3)	Coarse aggregate (kg/m^3)	Aggregate size (mm)	Super Plasticizer (kg/m^3)	
C20	0.75	304	229	990	862	4–14	–	24.5
C40	0.53	365	195	736	1117	4–14	–	33.7
C60	0.36	450	164	751	1088	5–16	5.9	51.2

Fig. 2. Concrete compression testing machine.

Fig. 3. Cylindrical concrete samples capped with sulphur.

of the measured strength owing to stress concentrations caused by irregularity of the surface. The mean compressive strength (f_{cm}) from each of the design mixes was determined as the average of six samples, and is presented in Table 3. Eq. (19) is used to obtain the characteristic

compressive strength (f_{ck}), in accordance with MC2010. It is noteworthy that the mean measured compressive strengths of concrete are quite less than the targeted values in some cases. This may be linked to the fact that cylindrical concrete sample provides lower compression strength compared with that of a cube.

3.2.2. Reinforcement

Austenitic stainless steel is the most common type of stainless steel material that is used for reinforcement owing to the excellent corrosion resistance and outstanding mechanical properties [1,2]; and therefore grade 1.4301 is selected in this study [31]. It is noteworthy that the austenitic stainless steel rebars used in this study are cold-rolled. Pull-out tests on carbon steel grade B500 [32] rebar are also conducted. In both cases, for the stainless and carbon steel tests, bars with a diameter of 10 mm and 12 mm are included. The geometrical details of the bars used in this study have been closely examined and measured, and the data is presented in Table 4.

The 12 mm stainless steel reinforcement bars are a version of grade 1.4301 reinforcement known as "grib-rib" which is available as high strength material [33]. This was not deliberately ordered as part of this study but is the default for 12 mm stainless steel rebar available in the UK. It comprise three series of transverse ribs around the bar cross-section rather than the typical two series which might enhance the bond performance. All of the carbon steel reinforcement bars used in this study consist of two series of transverse ribs at the cross-section and also two longitudinal ribs. Three repeat tests were carried out on each type of bar, and the average response is taken as a representative curve of a single specimen. The relative rib areas (f_p) presented in Table 4 are calculated using Eq. (1). It is noteworthy that the stainless steel and carbon steel reinforcements comply with the requirements given in BS 6744 [31] and BS 4449 + A3 [32], respectively, which are presented in Table 5, apart from the relative rib area for the 10 mm diameter stainless steel rebar which is found to be lower than the minimum required value.

3.3. Bond test arrangement

A total of 72 pull-out test samples were prepared and tested, in accordance with the guidance in EN 10080 [34], in two experimental programmes. The first phase comprised 60 tests (including 15 specimens for each reinforcement type and bar diameter) while the second phase consisted of 12 more samples including 3 tests for each reinforcement type and bar diameter. The programme included 5 and 3 repetitions of each specimen in phase 1 and phase 2, respectively and the average response is taken as a representative curve of a single specimen. A reference-system was adopted to label each specimen,

Table 4
Geometrical properties of the reinforcing bars.

Material	Bar diameter (mm)	Maximum Rib height (mm)	Rib spacing (mm)	Rib inclination (β)	F_P area of a single rib (mm^2)	Relative rib area (f_P)
Stainless steel	10	0.67	9.34	50°	5.74	0.030
Stainless steel (grib-rib)	12	0.75	7.58	55°	7.19	0.062
Carbon steel	10	1.03	6.85	55°	7.74	0.059
Carbon steel	12	1.16	7.04	60°	10.13	0.066

Table 5
Ranges for rib parameters for stainless steel [31] and carbon steel [32].

Rib height (mm)	Rib spacing (mm)	Rib inclination (β)	Min relative rib area for 10 and 12 mm bar diameter (f_P)
0.03d – 0.15d	0.4d – 1.2d	35 – 75°	0.04

Fig. 4. Rig used for the casting of the pull-out specimens.

where the first portion of the name denotes the type of rebar used (i.e. stainless steel (SS) or carbon steel (CS), the next term between the two hyphens defines the bar diameter (D10 for 10 mm and or D12 for 12 mm reinforcement), the third portion is the target concrete strength, whilst the last number refers to the phase of testing.

The moulds were fabricated from PVC material, as shown in Fig. 4. In the first phase of testing, each specimen was 110 mm in diameter and 120 mm in height. A single piece of rebar which was 500 mm in length was positioned at the centre of the specimen. The bonded length was set at 60 mm for all specimens, as shown in Fig. 5(b), so either 5 or 6 times the bar diameter, to reduce the effect of the longitudinal compressive stresses caused by bearing of the concrete against the plate that restrains the pull-out specimen [35]. The concrete was then cast in a vertical direction, and was compacted manually. All specimens were demoulded the day after casting and then cured in a water tank for 28 days. Fig. 5 presents a specimen in the testing machine as well as a schematic of the pull-out test arrangement. Two transducers were used to calculate the average steel-concrete slip at the passive side, as shown in the figure.

The second phase of testing was planned based on the results of the first phase, where splitting failure was prevalent (this will be discussed in more detail later). Accordingly, 12 more samples were prepared, each of which was 200 mm in length in order to avoid splitting failure. Cubic moulds were used in this phase due to unavailability of cylindrical moulds with a large enough diameter to avoid splitting of the concrete. In these samples, the bond length was set at 5 times the bar diameter and the overall bar length was 500 mm. As before, the stainless steel reinforcing bar was positioned in the centre of the specimen. The target concrete strength was 40 MPa and these specimens were cast in a horizontal direction and compacted using an electrical vibrator.

4. Test results

4.1. Tensile test results

Tensile tests have been conducted in order to obtain the stress-strain curves and the mechanical properties of both the carbon and stainless steel rebars, in accordance with EN 6892-1 [36], and the results are presented in Fig. 6 and Table 6, respectively. In Fig. 6, both the overall response is presented as well as a closer view of the elastic portion of

the behaviour. It is clear from the graph that the stainless steel and carbon steel rebars exhibit quite different stress-strain responses. The stainless steel specimens are much more ductile, with high ultimate strains and significant strain hardening, and also have a continuous curve without a clearly defined yield point. On the other hand, the carbon steel bars show a clear yield plateau followed by a moderate degree of strain hardening and limited ductility. In the absence of a visible yield point in stainless steels, the typical value adopted is the 0.2% proof stress.

With reference to the data presented in Table 6, the yield stress (f_y) for the stainless steels are 515 and 715 N/mm² for the 10 mm and 12 mm bars, respectively, where the equivalent values for the carbon steel rebars are 589 and 554 N/mm², respectively. The ultimate stress (f_u) for stainless steels are 19.6% and 36.8% higher than that of carbon steel for 10 mm and the 12 mm bars, respectively. As expected, the grib-rib stainless steel rebars exhibit the highest strength value among the others. Additionally, the stainless steel bars provide greater ductility than the carbon steel by around 159% and 129% for 10 mm and the 12 mm bars, respectively. It is also observed that the bars with diameter of 12 mm have lower ductility than those with diameter of 10 mm by around 35.0% and 26.3%. Moreover, the modulus of elasticity for stainless steel and carbon steel are quite similar, apart from the grib-rib stainless steel rebar which shows a lower modulus of elasticity compared to the equivalent carbon steel rebar.

4.2. Bond test results

Table 7 presents the pull-out test results, which reflect the average behaviour. In Table 7, the ultimate experimental bond strength (τ) is calculated using Eq. (21), where F is the ultimate applied load, l is the bonded length and ϕ is the diameter of the rebar:

$$\tau = \frac{F}{\pi \phi l} \tag{21}$$

Fig. 7(a) presents a specimen from test phase 1. All of the cylindrical specimens in this group failed by splitting, irrespective of the type or size of the reinforcement. This is mainly attributed to the insufficient confinement provided by the concrete as well as the relatively long bonded length compared to the total length of the specimen. On the other hand, pull-out failure was observed for all cubic specimens in Phase 2, as shown in Fig. 7(b), which were designed to provide more confinement.

Fig. 8 presents the bond-slip response for the bond tests conducted in Phase 1 of the test programme, for samples with (a) C20, (b) C40 and (c) C60 concrete, respectively. All of these specimens failed by splitting of the concrete. Generally, with reference to the graphs, it is observed that the stainless steel rebars exhibit lower ultimate bond strength compared to carbon steels by 28% on average. Similar conclusion is found in [24].

Fig. 9 presents the bond-slip response for the samples from Phase 2 of the bond test programme, all of which failed by pull-out failure. Similar to the earlier observations, it is again shown that stainless steels achieve lower ultimate bond strength values compared to carbon steel reinforcement, by around 40% on average. By comparing specimens with the same concrete strength and bar diameter from Phase 1 and 2, it is clear that the difference in ultimate bond strength between the samples with stainless steel and carbon steel reinforcement bars is even greater when pull-out failure occurs rather than splitting. In general, the samples with stainless steel exhibit a more rapid reduction of bond strength also in the softening stage compared to those with carbon steel, as well as lower residual bond values. It is observed in Fig. 9 that the bond response for samples with stainless steel rebar fluctuates in the post-peak range, which did not occur for either the carbon steel reinforced samples or those in Phase 1 which failed by splitting. This could be linked to the rib spacing in the reinforcement since it is observed that the distance between the two plateaus coincides with the rib
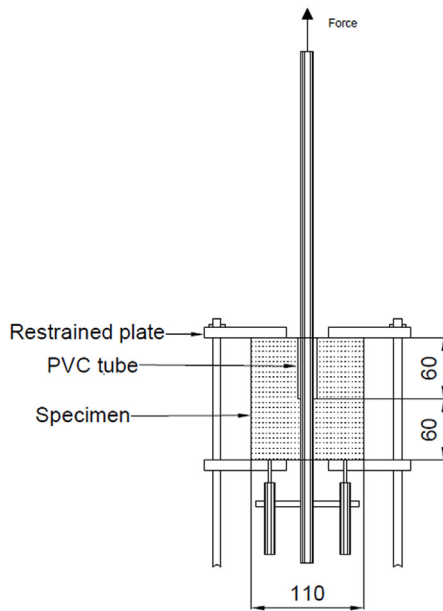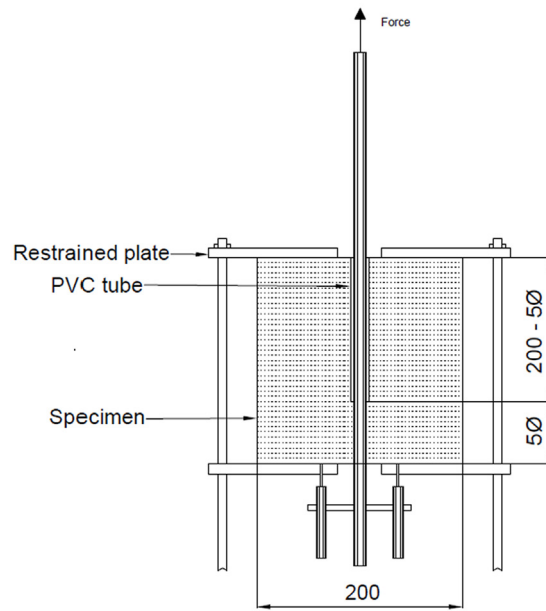
Fig. 5. Pull-out test arrangement including (a) an image of the testing machine, (b) a schematic of the pull-out set-up for Phase 1 and (c) a schematic of the pull-out set-up for Phase 2. All dimensions are given in mm.

spacing. In the following sub-sections, the tests results are further analysed and the impact of particular properties such as concrete strength, bar diameter and reinforcement material type are discussed.

4.2.1. Reinforcement material and diameter

It was observed in the previous section that stainless steel reinforcement bars achieve lower ultimate bond strength values compared with carbon steels, in all cases examined in the current

programme. In general, it is shown that the samples with stainless steel reinforcement bars had a relatively lower softening response compared to that of carbon steels in all cases except the specimen with 12 mm stainless steel and C60 concrete strength. Additionally, for the samples that experienced splitting failure, the bond that develops for the 12 mm stainless steel rebar is 35.2%, 27.8% and 25.1% lower than for carbon steel rebar for C20, C40 and C60, respectively. These same values for the 10 mm bars are 24.4%, 15.6% and 15%, respectively. These results
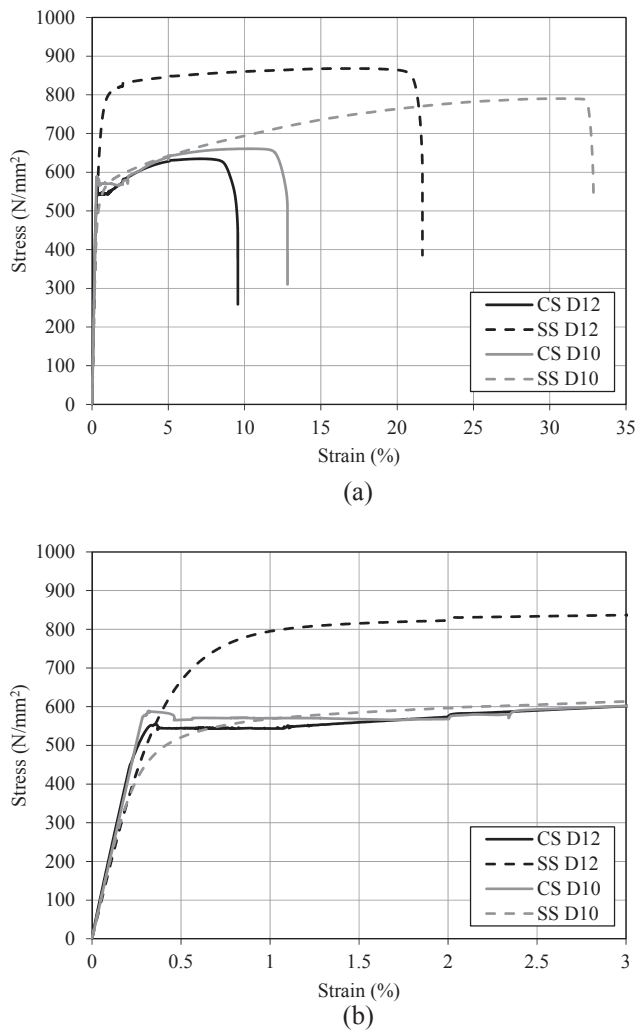
Fig. 6. Stress-strain curves of stainless steels and carbon steels (a) full curve and (b) more detailed view of the elastic region.

are in agreement with the findings in [24]. It is shown that for both bar diameters examined, the difference between stainless steel and carbon steel is greatest when the concrete strength is relatively low, i.e. for the samples with C20 concrete. This is most likely owing to the fact the stainless steels have lower relative rib areas than the carbon steel bars, and this influence is greater when the concrete strength is relatively low. Additionally, an increase in the water-to-cement ratio in the concrete mixture (i.e. lowering the concrete strength) results in lower alkalinity and thus greater porosity [37]. This illustrates how stainless steel reinforcement can be more beneficial than traditional carbon steel reinforcement for improving the durability of concrete structures.

It is also observed that using bars with a greater diameter increases the difference in the ultimate bond strength between stainless steel and carbon steel, in all cases in Phase 1. This is attributed to the fact that increasing the bar diameter from 10 mm to 12 mm enhances the ultimate bond strength for carbon steel by around 11% on average whereas

in contrast there is no considerable improvement for stainless steels or even results in lower bond strength in some particular cases. In contrast, for the samples that experienced pull-out failure in Phase 2, it is found that using bars with a greater diameter decreases the difference in the ultimate bond strength between stainless steel and carbon steel. It is observed that the bond strength for stainless steel increases by around 23% when the bar diameter changes from 10 mm to 12 mm. The equivalent value for carbon steel is just 1%. It is likely that the reason for this disparity is owing to the difference in the geometry of the samples used in Phase 1 and 2, including bonded length.

4.2.2. Concrete strength

Fig. 10(a) and (b) represent the influence that concrete strength has on the bond stress-slip behaviour for 10 mm stainless steel and carbon steel samples, respectively. The figures show that the samples with higher concrete strength exhibit greater bond strength, in all cases. For example, the ultimate bond strength that develops for 10 mm diameter samples with C60 concrete strength is improved by around 85% and 65% for stainless steel and carbon steel reinforcement bars, respectively, compared to those with C20 concrete strength. These same values for 12 mm bars are 89% and 63%. This conclusion is in line with the research findings reported by the International federation for structural concrete [12,13].

It is noteworthy to observe that the samples with concrete strength C40 and C60 generate relatively similar ultimate bond strength values with difference being around 5.4% and 4.6% for stainless steel and carbon steel reinforcement bars, respectively, as shown in Fig. 10. This indicates that the influence of concrete strength becomes less significant after a certain strength level. This observation is in line with the guidance given in Eurocode 2, where the design rules limit the bond strength to the value for C60/75 concrete strength class, unless it is verified that the average bond strength increases above this limit [16].

5. Comparison with design codes

5.1. Design bond strength, anchorage and lap lengths

Understanding the bond behaviour that develops between reinforcement and the surrounding concrete is imperative in the design of reinforced concrete structures, as it underpins the composite performance of the member. However, bond is a highly complex phenomenon that is influenced by many inter-related parameters which are difficult to measure and predict and therefore most global design standards provide quite conservative estimates for the bond strength that develops. In this context, the aim of this section is to evaluate the current design rules in Eurocode 2 (which will be referred as EC2) and MC2010 for reinforced concrete through comparison with the experimental results discussed previously, in terms of bond strength, anchorage length and lap length, as shown in Table 8. Both stainless steel and carbon steel are included in the analysis.

The experimental anchorage and lap lengths are obtained by substituting the experimental bond strength values into the appropriate Eurocode 2 design expressions without considering the minimum design values. It is noteworthy that the characteristic values for concrete and the reinforcement obtained experimentally and described in Section 3.2 are employed in this section in order to provide more

Table 6
Mechanical properties of the reinforcements.

Material	Diameter (mm)	Yield stress f_y (N/mm^2)	Ultimate strength f_u (N/mm^2)	Modulus of elasticity E (N/mm^2)	Ductility % (mm/mm)
Stainless steel	10	515	790	200,899	32.39
Stainless steel (grib-rib)	12	715	868	184,000	21.05
Carbon steel	10	589	661	201,368	12.49
Carbon steel	12	554	635	211,766	9.21

Table 7
Ultimate bond strength results of the pull-out tests.

Specimen	Mean measured compressive strength, f_{cm} (MPa)	Bar diameter, ϕ (mm)	Failure mode	Ultimate bond strength, τ (MPa)	Standard deviation	Difference in the ultimate bond strength, SS/CS (%)
SS-D10-C20-1	24.5	10	Splitting	12.1	0.75	−24.4
CS-D10-C20-1			Splitting	16.1	0.77	
SS-D12-C20-1		12	Splitting	12.0	0.49	−35.2
CS-D12-C20-1			Splitting	18.5	0.51	
SS-D10-C40-1	33.7	10	Splitting	21.3	1.56	−15.6
CS-D10-C40-1			Splitting	25.2	1.36	
SS-D12-C40-1		12	Splitting	18.9	1.19	−27.8
CS-D12-C40-1			Splitting	26.1	0.82	
SS-D10-C40-2	34.5	10	Pull-out	14.2	2.00	−46.1
CS-D10-C40-2			Pull-out	26.3	1.09	
SS-D12-C40-2		12	Pull-out	17.5	1.83	−34.3
CS-D12-C40-2			Pull-out	26.6	0.60	
SS-D10-C60-1	51.2	10	Splitting	22.4	1.28	−15.0
CS-D10-C60-1			Splitting	26.4	1.30	
SS-D12-C60-1		12	Splitting	22.7	0.59	−25.1
CS-D12-C60-1			Splitting	30.26	0.64	

realistic comparison. Since both codes predict bond strength on the basis of the characteristic values, the experimental bond results are presented here as the characteristic values which obtained using Eq. (19).

It is observed from the data presented in Table 8 that the design bond strength values predicted by both Eurocode 2 and MC2010 are very conservative when compared with the experimental ultimate bond strength values obtained in the current analysis. The Eurocode 2 bond strength predictions are around 49% and 73% less than the test values for stainless steel and carbon steel reinforcement, respectively, whereas the equivalent values for MC2010 are 59% and 78%, respectively. In all cases included in the current study, MC2010 is more conservative in its predictions of the design bond strength compared with Eurocode 2 with the average difference being around 19%.

With reference to the data in Table 8, it is observed that bond strength values obtained from Eurocode 2 for samples with stainless steel are identical to those with carbon steel for each concrete category irrespective of the bar size. On the other hand, in MC2010, it is observed that the difference in bond strength predictions between stainless steels and carbon steels are 13% and −19.6% on average for 10 mm and 12 mm bar diameter, respectively. As discussed in Section 2, the bond design rules in both codes are not influenced by the reinforcement type. Hence, this disparity in the prediction of bond is mainly because MC2010 takes into account the characteristic yield strength of the reinforcement and a higher reduction factor is applied for the rebar with greater characteristic yield strength. Since the 12 mm stainless steel rebar (grib-rib) has relatively higher strength property

compared with the other bars, a lower bond strength is predicted.

Similar conclusions are found for the design anchorage and lap lengths, as both Eurocode 2 and MC2010 provide extremely conservative anchorage and lap lengths compared with those calculated based on the experimental results. For instance, the anchorage lengths predicted using Eurocode 2 and MC2010 are higher than the experimental values by around 116% and 310% on average for stainless steel rebars and by around 281% and 570% for carbon steels, respectively. The equivalent values for the lap lengths are higher than the experimental results by around 134% and 310% on average for stainless steel rebars and by around 300% and 570% for carbon steel, respectively. It is clear that MC2010 is significantly more conservative than Eurocode 2, although it does take more of the influential material and geometrical properties in to account.

For 10 mm stainless steel, the anchorage lengths obtained using Eurocode 2 and MC2010 are lower than those for carbon steels by around 13% and 22% on average, respectively. On the other hand, the equivalent values for the 12 mm stainless steel are higher than those for carbon steels by 29% and 61%, respectively. Similar results are found for the lap lengths, as both Eurocode 2 and MC2010 require shorter lap lengths for the 10 mm stainless steel rebars compared with those for carbon steels by 7% and 22% on average. However, the codes require greater lap lengths for the 12 mm stainless steel rebars compared with those for carbon steels by 25% and 60% on average. As discussed earlier, the differences in the anchorage and lap lengths between stainless and carbon steel rebars are mainly attributed to the variations of the characteristic yield strength of the reinforcements.
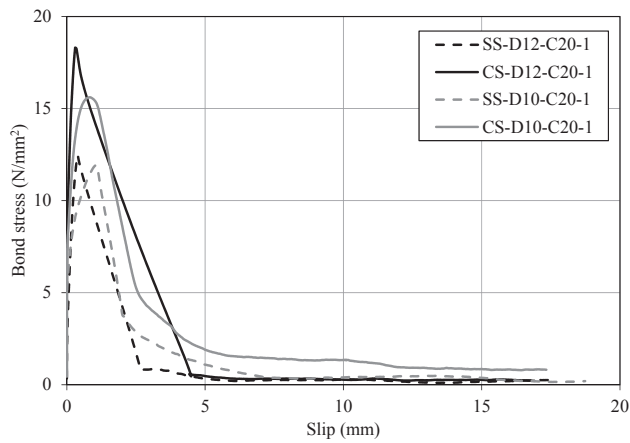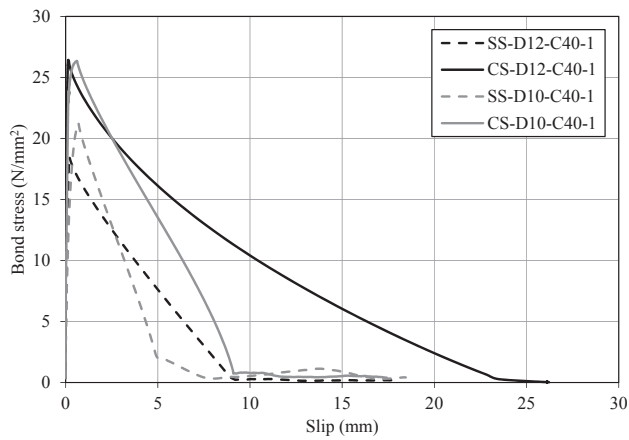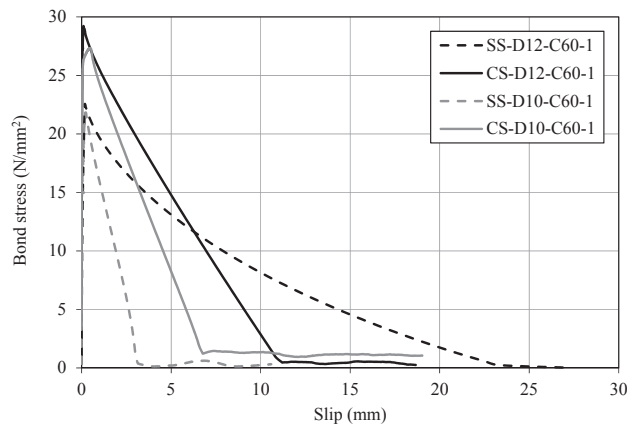

(a)

(b)

Fig. 7. Failure mode for specimens with stainless steel reinforcement from (a) phase 1-splitting failure and (b) phase 2-pull-out failure.

(a)

(b)

(c)

Fig. 8. Splitting bond stress-slip curves for carbon and stainless steel re-inforcements with concrete strength (a) 20 MPa (b) 40 MPa and (c) 60 MPa.

Fig. 9. Pull-out bond stress-slip curves for carbon and stainless steel re-inforcements with concrete strength 40 MPa.

(a)

(b)

Fig. 10. Bond stress-slip curves for samples with 10 mm bar diameter and concrete strengths C20, C40 and C60 for (a) stainless steel and (b) carbon steel rebar.

In conclusion, the design bond values given in both Eurocode 2 and MC2010 are shown to be very conservative compared with the ex-perimental results, even for the stainless steel reinforced concrete which was shown to have lower bond strength compared with regular carbon steel reinforced concrete. Therefore, it is concluded that the current design rules can be safely applied for stainless steel reinforced concrete structures, for the parameter range considered herein. However, the design codes provide inaccurate and inefficient predic-tions, mainly owing to the fact that they are not based wholly on fun-damental principles with all key parameters considered. In the
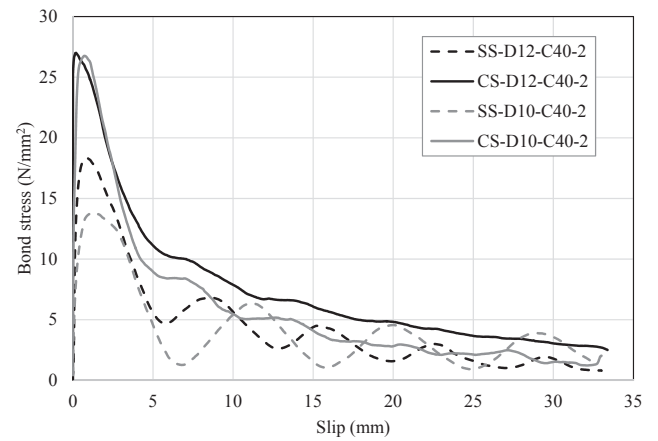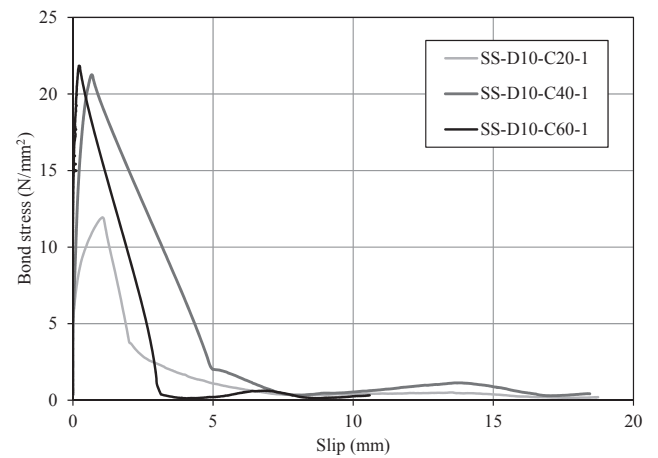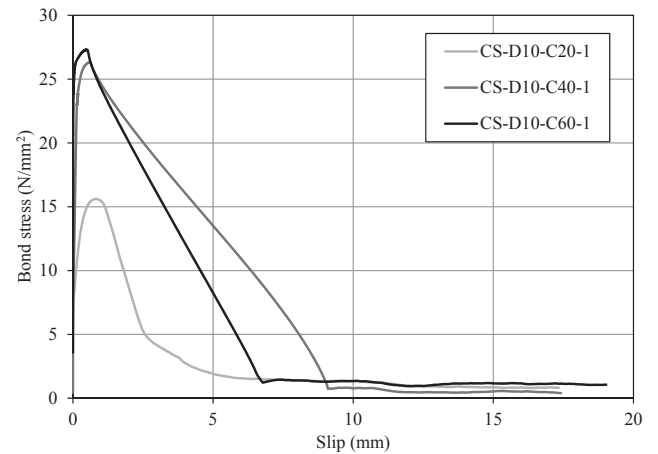
following sub-section, the design bond-slip model provided in the MC2010 is evaluated for the case of splitting and pull-out failure modes. Consequently, new bond-slip models are proposed for both stainless steel and carbon steel reinforced concrete.

Table 8
Results comparison with codes predictions.

Specimens	Mean measured compressive strength, f_{cm} (MPa)	Design bond strength, f_{bd} (MPa)			Design anchorage length, l_{bd} (mm)			Design lap length, l_0 (mm)		
		Exp	EC2	MC2010	Exp	EC2	MC2010	Exp	EC2	MC2010
SS-D10-C20-1	24.5	4.1	3.1	3.1	190	256	360	190	256	360
CS-D10-C20-1		8.1	3.1	2.8	111	293	464	111	293	464
SS-D12-C20-1		4.0	3.1	2.1	325	427	878	325	427	878
CS-D12-C20-1		10.5	3.1	2.6	96	331	547	96	331	547
SS-D10-C40-1	33.7	13.3	4.1	3.9	59	192	290	59	200	290
CS-D10-C40-1		17.2	4.1	3.4	52	219	373	52	219	373
SS-D12-C40-1		10.9	4.1	2.6	120	320	707	120	320	707
CS-D12-C40-1		18.1	4.1	3.3	56	248	441	56	248	441
SS-D10-C40-2	34.5	6.2	4.2	3.9	127	187	284	127	200	284
CS-D10-C40-2		18.3	4.2	3.5	49	213	365	49	213	365
SS-D12-C40-2		9.5	4.2	2.7	138	311	692	138	311	692
CS-D12-C40-2		18.6	4.2	3.3	54	241	431	54	241	431
SS-D10-C60-1	51.2	14.4	5.8	5.0	54	135	222	54	200	222
CS-D10-C60-1		18.4	5.8	4.5	49	154	286	49	200	286
SS-D12-C60-1		14.7	5.8	3.4	89	225	542	89	225	542
CS-D12-C60-1		22.3	5.8	4.3	45	174	338	45	200	338

5.2. Proposed bond stress-slip curve

The local bond stress-slip relationship is a key factor in design of reinforced concrete structures and has a significant influence on the crack propagation, stiffness and also integrity and resilience of members and frames. Owing to the previously-discussed complexity in analysing bond, and the variety of test conditions and structural applications, a large number of analytical models have been proposed in the literature to simulate the bond-slip response in reinforced concrete (e.g. [38–41]). The model which was presented by Eligehausen et al. [42] and then further developed for inclusion in MC2010 [17] incorporates a more simplistic solution and corresponds to the experimental behavior. Therefore, this model has been selected herein to evaluate the bond-slip response.

As discussed in the experimental analysis earlier in this paper, stainless steel rebars exhibit relatively lower bond strengths compared with carbon steel reinforcement. Hence, it is very imperative to examine the applicability of using the bond-slip model given in MC2010 for concrete members with stainless steel reinforcement. Since both pull-out failure and splitting failure were experienced in the tests, the bond-slip response is evaluated in terms of both failure modes. The results presented in this section are obtained for samples with C40 concrete strength. The details of the bond-slip model given in MC2010 are described previously in Fig. 1 using Eqs. (15)–(18) together with the parameters defined in Table 2.

Fig. 11 presents the bond-slip curves predicted using MC2010 for the splitting failure mode together with the corresponding experimental results, for samples with bar diameter of 10 mm and 12 mm. It is generally shown that the bond-slip response obtained using MC2010 underestimates the experimental response, in all cases, by quite some margin. It is clear that the current bond-slip model provided in the MC2010 for splitting failure mode does not reflect the actual behaviour for both stainless steel and carbon steel, for the test parameters studied herein.

It has been shown in this paper that the bond behaviour for stainless steel reinforced concrete is different to that of carbon steel reinforced concrete and therefore different bond-slip models are developed for each. The proposed curves for stainless steel and carbon steel are presented in Fig. 11 using Eqs. (15)–(18) together with the parameters defined in Table 9. The clear space between ribs (c_{clear}) is taken as 6 mm in all cases. It is evident from the data presented in Fig. 11 that the proposed curves provide a more accurate and representative depiction of the experimental behaviour in terms of the ascending branch, the ultimate bond strength and also softening range, in all cases. It is observed that implementing the proposed curves improves the ultimate
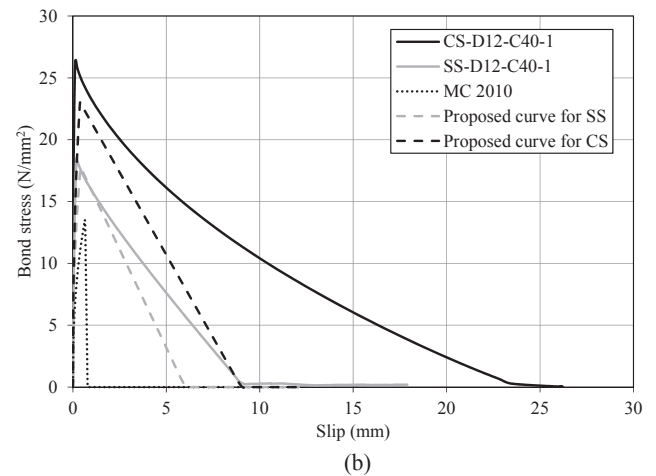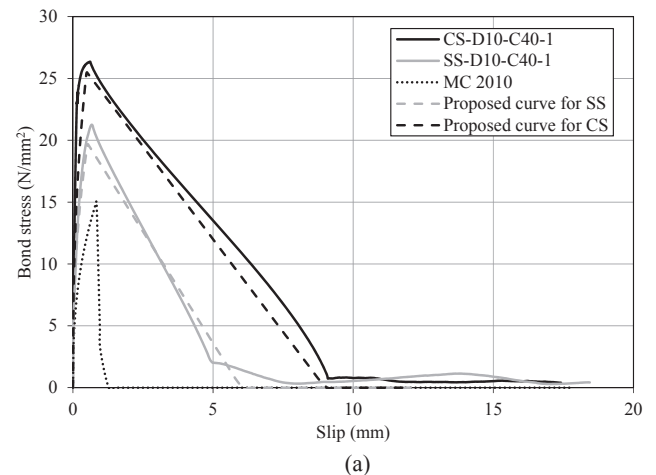

(a)

(b)

Fig. 11. Comparison of the experimental bond stress-slip curves and MC 2010 model for splitting failure mode for samples with reinforcement which is (a) 10 mm in diameter and (b) 12 mm in diameter.

bond strength by around 22% on average for stainless steel rebars and 38% for carbon steels.

In addition to the bond stress-slip relationship, the expression given in Eq. (20) previously for the ultimate bond strength for the splitting failure mode has been updated based on the analysis presented herein for stainless steel and carbon steel, as presented in Eqs. (22) and (23),

Table 9
Parameters details for the proposed splitting bond-slip model.

	Splitting failure (unconfined)		
	Current model in MC2010	Proposed model for stainless steel	Proposed model for carbon steel
τ_{bmax}	$2.5(f_{cm})^{0.5}$	$3(f_{cm})^{0.5}$	$4(f_{cm})^{0.5}$
$\tau_{bu,split}$	Eq. (20)	Eq. (22)	Eq. (23)
s_1	$s(\tau_{bu,split})$	$0.5\ s(\tau_{bu,split})$	$0.5\ s(\tau_{bu,split})$
s_2	s_1	s_1	s_1
s_3	$1.2\ s_1$	c_{clear}	$1.5c_{clear}$
α	0.4	0.4	0.4
τ_{bf}	0	0	0

respectively:

$$\tau_{bu,split} = 8.5\eta_2\left(\frac{f_{cm}}{25}\right)^{0.25}\left(\frac{25}{\phi}\right)^{0.2}\left[\left(\frac{C_{min}}{\phi}\right)^{0.33}\left(\frac{C_{max}}{C_{min}}\right)^{0.1} + k_m K_{tr}\right] \tag{22}$$

$$\tau_{bu,split} = 11\eta_2\left(\frac{f_{cm}}{25}\right)^{0.25}\left(\frac{25}{\phi}\right)^{0.2}\left[\left(\frac{C_{min}}{\phi}\right)^{0.33}\left(\frac{C_{max}}{C_{min}}\right)^{0.1} + k_m K_{tr}\right] \tag{23}$$

Fig. 12 presents the bond-slip curves predicted using the MC2010 for pull-out failure, together with the corresponding values from the experimental programme, for both stainless and carbon steel
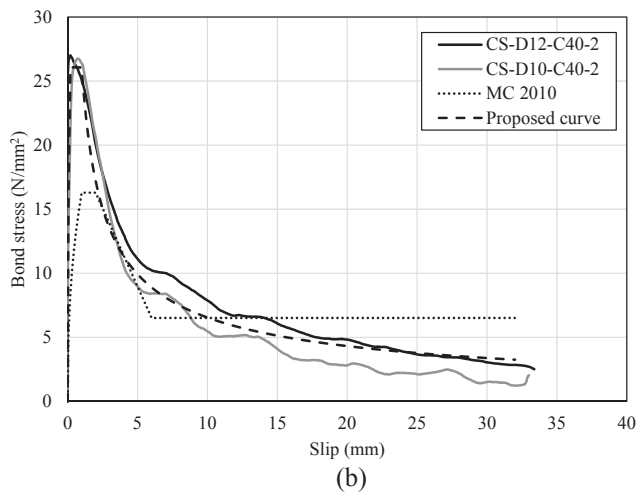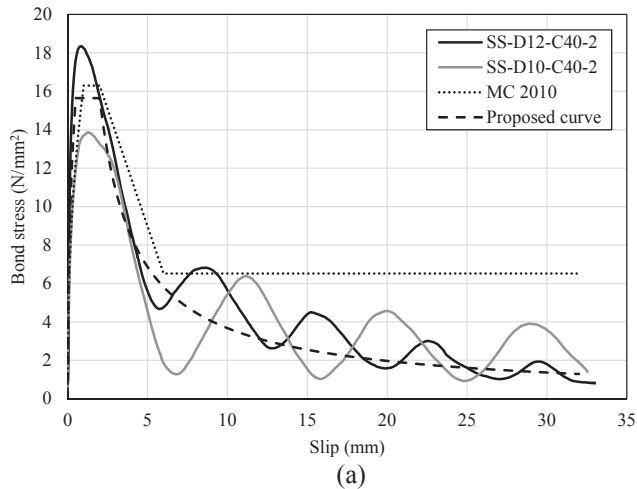
(a)

(b)

Fig. 12. Comparison of the experimental bond stress-slip curves and MC 2010 model for the pull-out failure mode for samples with (a) stainless steel and (b) carbon steel.
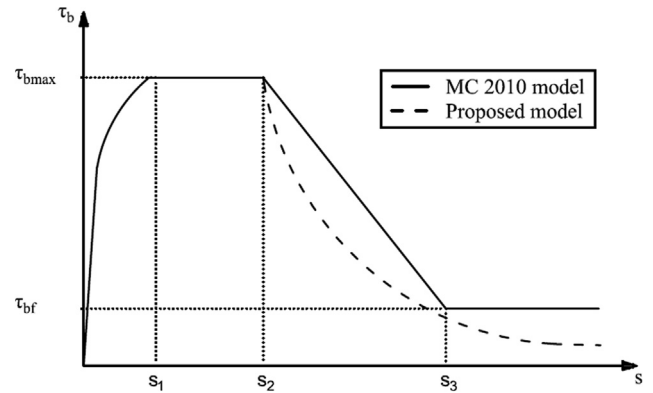
Fig. 13. Comparison of the proposed bond stress-slip model and the MC2010 model for pull-out failure mode.

reinforcement. Generally, it is clear that the MC2010 bond model does not reflect the actual bond-slip behaviour for either stainless steel or carbon steel reinforced concrete. For example, the MC2010 bond model results in a softer response in the ascending and descending branches and lower ultimate bond strength as well as an overestimation of the residual bond strength, compared with the experimental data. Moreover, the de-bonding part of the response is simulated in MC2010 as a linearly descending branch followed by constant level of the residual bond stress. It is very clear that this is quite different from the behaviour observed during the tests where the bond stress decreased gradually in an exponential manner.

The shape of the proposed bond model for the pull-out failure mode are presented in Fig. 13, together with the current model provided in MC2010. Since the post-peak region of the response has already been shown to be inaccurately represented by the MC2010, an exponential curve is implemented in order to reflect the experimental behaviour. The bond stress for the proposed model are calculated as a function of the relative displacement as given in Eqs. (24)–(26) and shown in Fig. 13. By comparing the proposed models with experimental responses, as presented in Fig. 12, it can be seen that the proposed models are in excellent agreement with experimental responses especially in the post-peak range, for both stainless steel and carbon steel reinforced concrete. It is believed that implementing these changes in the codes of practice will ensure providing more accurate and efficient design rules, which is extremely important for all structures, but particular those containing stainless steel reinforcement owing to its high initial cost.

$$\tau_b = \tau_{bmax}(s/s_1)^\alpha \quad \text{for} \ \ 0 \le s \le s_1 \tag{24}$$

$$\tau_b = \tau_{bmax} \quad \text{for} \ \ s_1 \le s \le s_2 \tag{25}$$

$$\tau_b = \tau_{bmax}(s_2/s)^{\alpha_1} \quad \text{for} \ \ s_2 \le s \tag{26}$$

The parameters in these expressions are defined in Table 10.

Table 10
Parameters details for the proposed pull-out bond-slip model.

	Pull-out failure		
	Current model in MC2010	Proposed model for stainless steel	Proposed model for carbon steel
τ_{bmax}	$2.5(f_{cm})^{0.5}$	$2.4(f_{cm})^{0.5}$	$4(f_{cm})^{0.5}$
s_1	1.0 mm	0.5	0.2
s_2	2.0 mm	2	1
s_3	c_{clear}	–	–
α	0.4	0.4	0.4
α_1	–	0.9	0.6
τ_{bf}	$0.4\tau_{bmax}$	–	–

6. Conclusions

Stainless steel reinforcement is receiving increasing attention from the construction sector, in response to the ever-increasing demands for structures and infrastructure to be more resilient, durable and efficient compared with traditional designs. The bond study presented herein fills significant knowledge gaps and enables stainless steel reinforcement bars to be specified in design with more confidence. This paper presents a detailed analysis of the bond behaviour between stainless steel reinforcement and the surrounding concrete, including both experimental and design analysis. Following this detailed study, the following key findings and recommendations for international codes of practice are presented:

- For the range of data examined here, it is observed that the stainless steel rebars exhibit lower ultimate bond strength compared with that of carbon steels by around 28% on average.
- In general, the samples with stainless steel exhibit a more rapid reduction of bond strength in the softening range compared to those with carbon steel, as well as lower residual bond values in the case of pull-out failure.
- It is shown that the samples with relatively higher concrete strength exhibit greater bond strength. However, the influence of concrete strength becomes less significant after a certain strength level.
- The design bond values given in both Eurocode 2 and MC2010 are shown to be very conservative compared with the experimental results, even for the stainless steel reinforced concrete.
- It is concluded that the current design rules can be safely applied for stainless steel reinforced concrete structures, for the parameter range considered herein. However, the design codes provide inaccurate and inefficient predictions, mainly owing to the fact that they are not based wholly on fundamental principles with all key parameters considered.
- It is generally shown that the bond-slip response obtained using MC2010 underestimates the experimental response, in all cases, by quite some margin, which does not reflect the actual behaviour for both stainless steel and carbon steel, for the test parameters studied herein.
- The post-peak region of the response has already been shown to be inaccurately represented by the MC2010, therefore it is suggested to implement an exponential curve in order to reflect the experimental behaviour.
- Consequently, new bond-slip models with calibrated design parameters are proposed for both stainless steel and carbon steel reinforced concrete, to accurately depict the true behaviour.

Declaration of Competing Interest

The authors declare that they have no known competing financial interests or personal relationships that could have appeared to influence the work reported in this paper.

Appendix A. Supplementary material

Supplementary data to this article can be found online at https://doi.org/10.1016/j.engstruct.2020.111027.

References

[1] Baddoo R, Burgan A. 'Structural Design of Stainless Steel', SCI Publication No. P291. The Steel Construction Institute; 2012.
[2] Gardner L. The use of stainless steel in structures. Prog Struct Mat Eng 2005;7(2):45–55.
[3] Rabi M, Cashell KA, Shamass R. Analysis of concrete beams reinforced with stainless steel. Proceedings of the fib symposium 2019: concrete-innovations in materials, design and structures. 2019. p. 690–7.
[4] Evans K.'RB Rebak in Corrosion Science–A Retrospective and Current Status in Honor of Robert P', Frankenthal, PV, 13; 2002. p. 344–54.
[5] Helland S. Design for service life: implementation of fib Model Code 2010 rules in the operational code ISO 16204. Struct Concrete 2013;14(1):10–8.
[6] British Stainless Steel Association. 'The use of stainless steel reinforcement on bridges'; 2003. Available at: http://www.bssa.org.uk/cms/File/REBar%20report.pdf [accessed: 11 April 2017].
[7] Calderon-Uriszar-Aldaca I, Briz E, Larrinaga P, Garcia H. Bonding strength of stainless steel rebars in concretes exposed to marine environments. Constr Build Mater 2018;172:125–33.
[8] Val DV, Stewart MG. Life-cycle cost analysis of reinforced concrete structures in marine environments. Struct Saf 2003;25(4):343–62.
[9] Cramer S, Covino B, Bullard S, Holcomb G, Russell J, Nelson F, et al. Corrosion prevention and remediation strategies for reinforced concrete coastal bridges. Cem Concr Compos 2002;24(1):101–17.
[10] Rabi M, Cashell K, Shamass R. Flexural analysis and design of stainless steel reinforced concrete beams. Eng Struct 2019;198:109432.
[11] Gardner L, Bu Y, Francis P, Baddoo NR, Cashell KA, McCann F. Elevated temperature material properties of stainless steel reinforcing bar. Constr Build Mater 2016;114:977–97.
[12] Balazs G, Cairns J, Eligehausen R, Lettow S, Metelli G, Pantazopoulou S, et al. Bond and anchorage of embedded reinforcement: background to the fib model code for concrete structures 2010. Bulletin 2014; 72: 7.
[13] Gambarova P, Balazs G, Vliet AB, Cairns J, Eligehausen R, Engstrom B, et al. Bond mechanics including pull-out and splitting failures. Bulletin - Fédération internationale du béton 2000. p. 1–97.
[14] EN 15630-1. Steel for the reinforcement and prestressing of concrete. Test methods Part 1: Reinforcing bars, wire rod and wire. European Committee for Standardization (CEN); 2010.
[15] Darwin D, Graham EK. Effect of deformation height and spacing on bond strength of reinforcing bars. ACI Struct J 1993;90(6):646–57.
[16] EN 1992-1-1. Eurocode 2: Design of concrete structures part 1-1: General rules and rules for buildings. European Committee for Standardization (CEN); 2004.
[17] Fédération Internationale du Béton. Fib Model Code for Concrete Structures 2010. Berlin: Wilhelm Ernst & Sohn Verlag fur Architektur und Technische; 2013.
[18] Bautista A, Blanco G, Velasco F, Gutiérrez A, Palacín S, Soriano L, et al. Passivation of duplex stainless steel in solutions simulating chloride-contaminated concrete. Materiales de Construcción 2007;57(288):17–32.
[19] Alvarez SM, Bautista A, Velasco F. Corrosion behaviour of corrugated lean duplex stainless steels in simulated concrete pore solutions. Corros Sci 2011;53(5):1748–55.
[20] Serdar M, Žulj LV, Bjegović D. Long-term corrosion behaviour of stainless reinforcing steel in mortar exposed to chloride environment. Corros Sci 2013;69:149–57.
[21] Lollini F, Carsana M, Gastaldi M, Redaelli E. Corrosion behaviour of stainless steel reinforcement in concrete. Corros Rev 2019;37(1):3–19.
[22] Van Niejenhuis CB, Walbridge S, Hansson CM. The performance of austenitic and duplex stainless steels in cracked concrete exposed to concentrated chloride brine. J Mater Sci 2016;51(1):362–74.
[23] Zhou Y, Ou Y, Lee GC. Bond-slip responses of stainless reinforcing bars in grouted ducts. Eng Struct 2017;141:651–65.
[24] Aal Hassan A. Bond of reinforcement in concrete with different types of corroded bars. Master Thesis. Toronto: Reyerson University; 2003. p. 106.
[25] Ahlborn T, DenHartigh T. Comparative bond study of stainless and high-chromium reinforcing bars in concrete. Transp Res Rec: J Transp Res Board 2003;1845:88–95.
[26] Johnson JB. Bond strength of corrosion resistant steel reinforcement in concrete. Master of Science in Civil Engineering, Faculty of the Virginia Polytechnic Institute and State University; 2010.
[27] RILEM. Technical recommendations for the testing and use of construction materials. Taylor & Francis, London; 1994.
[28] Shen D, Shi X, Zhang H, Duan X, Jiang G. Experimental study of early-age bond behavior between high strength concrete and steel bars using a pull-out test. Constr Build Mater 2016;113:653–63.
[29] Wei W, Liu F, Xiong Z, Lu Z, Li L. Bond performance between fibre-reinforced polymer bars and concrete under pull-out tests. Constr Build Mater 2019;227:116803.
[30] EN 12390-3. Testing hardened concrete Part 3: Compressive strength of test specimens. European Committee for Standardization (CEN); 2009.
[31] BS 6744.Stainless steel bars for the reinforcement of concrete. Requirements and test methods. British Standards Institution; 2016.
[32] BS 4449 + A3. Steel for the reinforcement of concrete. Weldable reinforcing steel. Bar, coil and decoiled product. Specifications, British Standards Institution; 2005.
[33] Stainless UK. Stainless Steel reinforcing bar; 2016. Available at: https://www.stainless-uk.co.uk/products/rebar/ [accessed: 07/30 2019].
[34] BS EN 10080. Steel for the reinforcement of concrete– Weldable reinforcing steel–General. British Standards Institution; 2005.
[35] Carvalho EP, Miranda MP, Fernandes DS, Alves GV. Comparison of test methodologies to evaluate steel-concrete bond strength of thin reinforcing bar. Constr Build Mater 2018;183:243–52.
[36] EN 6892-1. Metallic materials- Tensile testing part 1: Method of test at room temperature. European Committee for Standardization (CEN); 2016.
[37] Al-Kheetan, MJ, Rahman MM, Ghaffar SH, Al-Tarawneh M, Jweihan YS. Comprehensive Investigation of the Long-term Performance of Internally Integrated Concrete Pavement with Sodium Acetate. Res Eng; 2020: 100110.
[38] Nilson AH. Nonlinear analysis of reinforced concrete by the finite element method. J Proc 1968:757–66.
[39] Somayaji S, Shah SP. bond stress versus slip relationship and cracking response of tension members. J Am Concrete Inst 1981;78(3):217–25.
[40] Harajli M, Hout M, Jalkh W. Local bond stress-slip behavior of reinforcing bars embedded in plain and fiber concrete. Mater J 1995;92(4):343–53.
[41] Oh BH, Kim SH. Realistic models for local bond stress-slip of reinforced concrete under repeated loading. J Struct Eng 2007;133(2):216–24.
[42] Eligehausen R, Popov EP, Bertero VV. local bond stress-slip relationships of deformed bars under generalized excitations 1982; (4): 69–80.